Numerical Simulation of Sediment Movement and Deposition in a Meandering Channel

USMAN GHANI*, PETER RICHARD WORMLEATON**, AND ABDUL RAZZAQ GHUMMAN***

RECEIVED ON 22.12.2009 ACCEPTED ON 08.06.2010

ABSTRACT

In this research work, predictions have been made for the transport and deposition of incoming sediments in an open channel. Attempt has been made to understand the behavior of sediments flowing in the channel. The geometry consisted of a meandering compound channel with a constant inflow of sediments. For this purpose, 3D version of CFD (Computational Fluid Dynamics) code FLUENT has been used as a research tool. The turbulence closure of Reynolds Averaged Navior-Stokes equation was performed with standard - turbulence model. The Lagrangian particle tracking technique available in the code has been used for modeling sediment movement and deposition. For this purpose, nine different ranges of the particle diameters were released at the inlet of the channel. Initially, the model was validated using point velocities in the downstream direction and discharge values at five cross sections along the meander wavelength. The channel used for simulation purposes had a rectangular section. Once the model validated, it was then used for simulation of sediments. The numerical modeling gave a detailed picture of sediment deposited and transported through the channel. As the model was used with - turbulence model and Lagrangian particle tracking technique and then validated, it showed that when this combination of particle tracking and turbulence closure option will be used, the prediction will be fairly good and trustworthy. A number of numerical experiments were conducted to get the impact of sediment inflow velocity and its diameter on deposition patterns. It showed that boundary shearing stresses and secondary flows had considerable impact on sediment deposition in a river bend. The current study revealed that CFD technique can be used for predicting sediment distribution patterns with reasonable confidence. Such prediction techniques are not only economical but also provide details of complex flow and sediment movement behavior which are difficult to get through experimentation. The results predicted can be utilized in handling the deposition and erosion of the sediments in the meandering channels and design of natural and man-made meandering channels can be improved. It will also be helpful in designing proper flushing arrangements of deposited sediments.

Key Words: **Numerical Simulation, Sediment Deposition, Point Velocities, Lagrangian Particle Tracking Technique, Sediment Inflow.**

1. INTRODUCTION

When river discharge levels are high, floodplains on both sides of the river may become inundated. The floodplains then act as conveyance zones or as flood water storage basins. These floodplains are laden with high concentration of suspended sediments during floods. The sediments are transported into the floodplains from the main channel due to convection and diffusion processes where they

* Assistant Professor, Department of Civil Engineering, University of Engineering & Technology, Taxila.
** Senior Lecturer, Department of Engineering, Queen Mary, University of London, Mile End Road, London.
*** Professor, Department of Civil Engineering, University of Engineering & Technology, Taxila.

are deposited in the regions of low flow velocity. The investigations into the sedimentation in the main channel and over the floodplains have been done to a reasonable extent in the past using physical models and field experiments [1-3]. However, the study of sediment behavior within the meandering compound channels using 3D CFD techniques is yet being conducted and a lot more is required. The CFD techniques are cost effective against laboratory experiments, field observations and help us to have a detailed insight into sediment deposition and erosion behavior. The CFD methodology also consumes much less time for producing the results comparable to laboratory experimentation.

The physical phenomenon which controls the sediment transport in rivers is very important in various engineering problems. In river flows, the interaction between water and sediments results in a complicated mechanism and needs to be investigated thoroughly. At the earlier stages, these were investigated using 2D-depth averaged numerical models [4]. The river flows are turbulent and thus result in re-suspension, settlement and transfer of sediments. Recent advances in 3D CFD models have helped a lot to study this complex behavior of sediments in compound channels. A number of researchers [5-7] used different turbulence models and large eddy simulation technique to get 3D flow behavior in meandering rivers.

As far as bed load transport is concerned, most of the earlier studies were based upon semi-empirical equations. However, semi-empirical approaches failed to give true physical phenomena controlling their behavior. Sediment transport involves two phase liquid-solid flow. It needs a two phase flow model for transport analysis. A number of researchers have used a two phase flow model approach in which sediments were taken as second phase. The initial attempts for considering the two phase sediment flow mixture was based on a dispersion model which treats the particles as a transferable scalar. However dispersion model does not account for full interaction between particles and turbulent behavior of flow. To overcome this draw back of the existing models, various researchers [8-9] developed a model for simulating the particle deposition using Lagrangian particle trajectory technique.

In this research work, the numerical code FLUENT [10] has been utilized with Lagrangian particle tracking option to simulate the sediment deposition process in a meandering compound channel. The model was first validated using experimental data of primary depth averaged velocities and discharge values at various cross sections along the meander wavelength. Once the validation process was completed, the model was then used for simulation of sediment deposition across the channel. The turbulence closure was done using standard - turbulence model. The log law and standard wall function has been used to resolve the velocity gradients in the viscous sublayer close to the wall boundaries.

The study provides us an insight into the behavior of sediments, their deposition and movement. It gives us an opportunity to decide the capability of FLUENT code for sediment tracking when used with - turbulence model.

2. NUMERICAL CODE: FLUENT

FLUENT uses finite volume approach to solve 3D incompressible continuity and Reynolds-averaged Navior-Stokes equations. Different types of discretization schemes (QUICK, MUSCL, First Order upwind scheme, Second Order upwind scheme, hybrid) are available in it. A number of turbulence models such as k-ε, RNG k-ε, k-ω, Reynolds stress model etc. are offered by this numerical code. This code gives a number of options for simulation of two phase flow including Lagrangian particle tracking technique, Discrete phase modelling, Eulerian-Eulerian two phase modelling technique etc. This code is widely used in all areas of fluids such as mechanical, chemical, petroleum, environmental engineering etc. In Civil engineering, it is used in open channel and pipe flows. It is used for all types of external and internal flow cases. Its validity is being enhanced with the passage of time. It has the option of user defined function swhich one can incorporate his/her own code. For example if a boundary condition is not available in FLUENT, the modeller can incorporate the desired one using C-language programming. The custom field function option of this code offers insertion of a variety of mathematical relationships in the main programme during post-processsing. The pressure velocity coupling can be done using SIMPLE, SIMPLER, SIMPLEC and PISO algorithms. The case considered here is a steady state flow with general flow equations in Cartesian coordinates as:

Continuity Equation

$$\frac{\partial U_i}{\partial x_i} = 0 \tag{1}$$

Momentum Equation

$$U_j \frac{\partial}{\partial x_j}(U_i) = \frac{\nu}{\rho}\frac{\partial}{\partial x_j}\left(\frac{\partial U_i}{\partial x_j} + \frac{\partial U_j}{\partial x_i}\right) - \frac{1}{\rho}\frac{\partial P}{\partial x_i} + F_i + \left(-\overline{u_i u_j}\right) \tag{1}$$

Different terms in these equations are as follows. P is the pressure, ν and ρ are the kinematic viscosity and density of the water respectively, U_i is the time-averaged velocity component in x_i direction, F_i denotes external force (gravity forces), and $u_i u_j$ are the Reynolds stresses which result from the decomposition of instantaneous velocities into their mean and fluctuating components. The Reynolds stresses are expressed as:

$$-\overline{u_i u_j} = \nu_t\left(\frac{\partial U_i}{\partial U_j} + \frac{\partial U_j}{\partial U_i}\right) - \frac{2}{3}k\delta_{ij} \tag{3}$$

The ν_i in this equation is known as eddy viscosity, k and δ_{ij} are turbulent kinetic energy and Kronecker delta respectively.

$$\nu_t = c_\mu \frac{k^2}{\varepsilon} \tag{4}$$

Where c_μ is a constant. The turbulent kinetic energy k and its dissipation rate ε are calculated from the following transport equations:

$$U_i \frac{\partial k}{\partial x_i} = \frac{\partial}{\partial x_i}\left(\frac{\nu_t}{\sigma_k}\frac{\partial k}{\partial x_i}\right) + P_k - \varepsilon \tag{5}$$

$$U_i \frac{\partial \varepsilon}{\partial x_i} = \frac{\partial}{\partial x_i}\left(\frac{\nu_t}{\sigma_\varepsilon}\frac{\partial \varepsilon}{\partial x_i}\right) + \frac{\varepsilon}{k}\left(c_{1\varepsilon}P_k - c_{2\varepsilon}\varepsilon\right) \tag{6}$$

In these equations c_μ, σ_k, σ_ε, $c_{1\varepsilon}$, $c_{2\varepsilon}$ are empirical constants. Their values are as under [11]:

$c_\mu = 0.09,\ \sigma_k = 1.0, \sigma\varepsilon = 1.3, s_{\varepsilon 1} = 1.44, s_{\varepsilon 2} = 1.92$

The equation of motion of sediments is given by:

$$\frac{du_i^p}{dt} = \frac{3\nu C_D \mathrm{Re}_p}{4d^2 S}(u_i - u_i^p) + g_i \text{ and } \frac{du_i}{dt} = u_i^p$$

where μ^p_i is the velocity of the particle and x_i is its position, g_i is the acceleration due to gravity, S is the ratio of particle density to fluid density (the ratio has been taken as 2.65), d is the particle diameter (only disc type particles have considered), and m is the mass of the particle.

3. PHYSICAL MODEL DESCRIPTION

The experimental results used in this work were obtained from Martin Marriott's experiments at the University of Hertford [12].

The planform consisted of a meandering rectangular main channel made up of centre line circular arcs with a radius of 500mm and included angle of 140º joined tangentially at the cross over points. The resulting sinuosity was 1.3. The important dimensions of the channel and floodplains are as in Fig. 1 (a-b) Table 1.

The following boundary conditions have been applied in this case.

(i) At the inlet, the velocity distribution and turbulence properties i.e. k (turbulence kinetic energy) and ε (turbulence dissipation rate) have been specified.

(ii) At the outlet, the fixed pressure condition was given as the boundary condition and pressure was fixed as zero.

(iii) At the channel and floodplain boundaries, no slip condition was applied. In it the logarithmic law has been used and standard wall function was employed to resolve velocity gradients in the viscous sub-layer close to the walls.

(iv) Whilst, the free surface has been taken as an axis of symmetry which has been achieved by assuming a rigid lid on the free surface. As a result volume of fluid approach need not be used for simulating this case. This planar rigid lid acts as the plane of symmetry, normal gradients of all the variables except dissipation rate of turbulent kinetic energy. Normal velocity is also zero on this axis [13-14].

4. SOLUTION SEQUENCE

To solve Reynolds-averaged Navier-Stokes equations a number of solution technique and numerical control parameters are to be chosen. The residual values for different variables were set as $1x10^{-6}$. The calculation was initiated using the default under-relaxation coefficients provided in the Fluent 6.3. All other parameters are as shown in Table 2.

5. MESH GEOMETRY

An unstructured tetrahedral mesh was used to discretize the geometry for simulation on GAMBIT [15]. The mesh used had the following node numbers 201x15x10 in the main channel. As we are more interested in calculation of flow parameters within and close to the channel boundaries as compared to floodplain, the mesh was made fine in these areas and gradually coarsened as we moved away from the channel. As a result a mesh of 201x36x6 was used in the floodplain. The lateral grid sizes on the floodplains decreased gradually from the outer floodplain edge to the main channel bank. For checking the grid dependency the number of nodes was doubled in all three directions i.e. x, y, and z turn by turn. Different meshes tested are shown in Table 3 and results obtained for depth averaged velocities at the apex E using these meshes have been shown in Fig. 2. The largest absolute mean difference in velocity components through doubling the node numbers was small enough so that results can be termed as grid independent. A post processing check on mesh quality based on assessing the skewness of the generated mesh elements indicated that the mesh is of high quality and

FIG. 1(b). 3D VIEW OF EXPERIMENTAL CHANNEL

Table 1. Different parameters of the input data used in this paper

Experimental Reference	Discharge (l/sec)	Depth Over Floodplain (mm)	Floodplain Slope	Roughness (mm)
111	25.6	159	0.00142	0.00414

TABLE 2. VARIOUS OPTIONS USED IN THIS SIMULATION WORK

Model: Segregated	
Space	Three Dimensional
Time	Steady
Turbulence	Standard k-ε Model
Discretization Method	
Pressure	Standard
Pressure-Velocity Coupling	Simpler
Momentum	First-Order Upwind
Turbulence Kinetic Energy	First-Order Upwind
Turbulence Dissipation Rate	First-Order Upwind

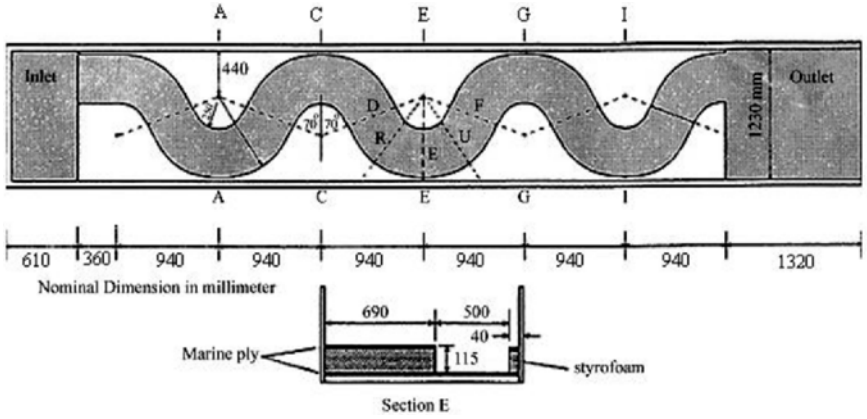

FIG. 1(a). THE GEOMETRY USED IN THIS STUDY SHOWING DIFFERENT ASPECTS OF THE CHANNEL.

would not compromise solution stability. The final mesh used for simulation work has been shown in Fig.3. The validation of the results obtained through this final mesh has been established by comparing simulated results of discharge and point velocities with experimental values in Section 6.1.1.

6. RESULTS AND DISCUSSION

6.1.1 Model Validation

The performance of the numerical code was validated using the experimental data of point velocities in downstream direction at the apex E and discharge values along the main channel. The same values were calculated with the help of FLUENT and results were compared as shown in Figs. 4-5. The experimental and simulated values match very closely. The RMS value for calculated and observed discharge values was within 6%. Similarly the relative %age error between the predicted and observed point velocities in downstream direction remained below 8%. It was therefore, concluded that the numerical code can be used for simulating the sediment deposition in the meandering channels.

TABLE 3. DIFFERENT MESHES TESTED

Mesh Size (on Floodplains)	Mesh Refinement
201x36x6	Final Used Mesh
201x72x6	Node Values Doubled in y Direction
201x72x12	Node Values Doubled in y, z Directions
201x36x12	Node Values Doubled in z Direction
402x36x6	Node Values Doubled in x Direction

6.1.2 Sediment Transport and Deposition

As the capability of the numerical code to predict the flow behavior is quite well (with RMS value of 6% for discharge calculations and less than 8% for point

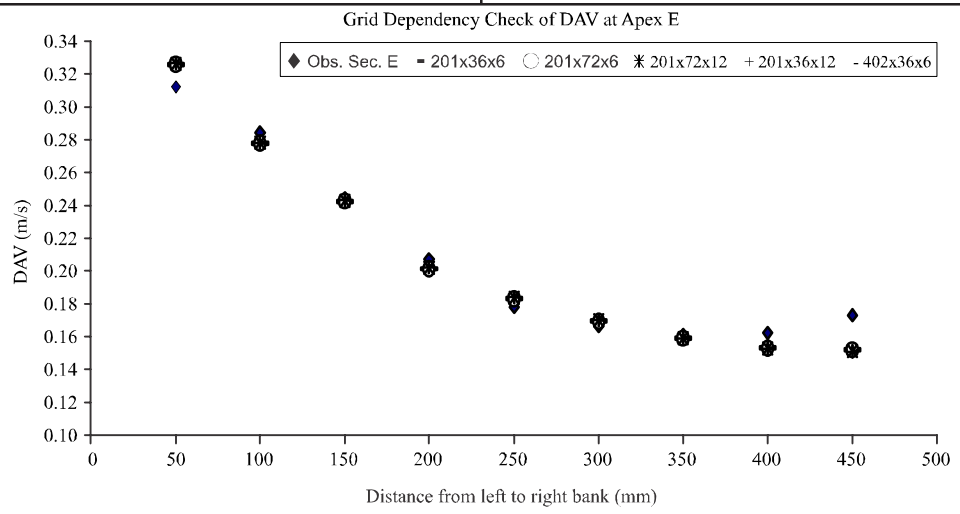

FIG. 2. GRID DEPENDENCY CHECK OF DAV AT APEX E OF 111 USING FIVE GRIDS

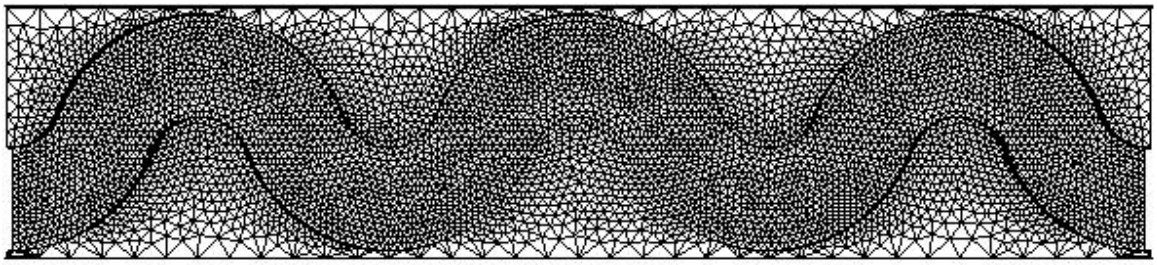

FIG. 3. MESH USED IN THE SIMULATION WORK

velocities as described in previous section), it was then used for simulation of sediment transport and deposition. For this purpose the apex E of the geometry shown in Fig.1(a) was selected as the critical section. In this work, the percentage of sediments deposited across the channel was obtained. Nine different sediment diameter ranges used in this study include 1-4, 4-8, 8-16, 16-31, 31-62, 62-125, 125-250, 250-500 and 500-1000μm. In this simulation work, 15,000 particles of any particular diameter range of the sediments were incorporated in the flow channel at the inlet and their flow trajectories were analysed. The initial distribution of these sediment particles was assumed to be uniform at the inlet of the flume. Simulations were conducted for three different inlet velocities. The velocity values were 1 m/sec, 1.5 m/sec and 2 m/sec. The deposition of the sediments was observed at one particular cross section for all cases. The percentage of these sediment particles which were deposited on the channel bed (trap efficiency) was then calculated and sketched against the width of the channel. The particles distribution patterns were calculated across the channel width at 50mm distances for each diameter range. Each distribution pattern in the graph corresponds to a particular velocity value. The numerical simulation of these sediment deposition patterns was done through Lagrangian particle tracking approach available in the multiphase flow models of the FLUENT software package.

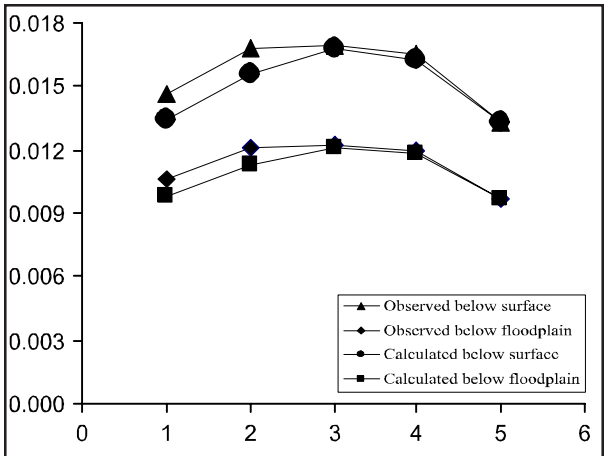

FIG. 4. DISCHARGE CALCULATIONS: THE HORIZONTAL AXIS INDICATES THE X-SECTIONS FROM LEFT TO RIGHT ALONG THE MEANDER WAVELENGTH (1, 2, 3, 4, 5 MEANS X-SECTIONS D, R, E, U, F SHOWN IN FIG. 1. VERTICAL AXIS INDICATES DISCHARGE IN m^3/SEC.)

Fig. 6(a) shows the deposition percentage of the particles in the range of 1-4μm range. As these are very small sized particles, therefore, the percentage deposited was very low and it is very clear from this diagram that most of the particles remained suspended and left the channel without considerable deposition. The percentage deposition was more towards the sides of the channel than the inner parts. This might be due to low velocity profiles and viscous effects towards the walls of the channel. Another result obtained from Fig. 6(a) is that the sediment deposition was low for high velocity magnitude (1.5 m/sec) and greater for low inlet velocity (1 m/sec). Fig. 6(b) gives us the particle distribution pattern with diameters in the range 4-8μm. A close examination of this diagram indicates that particle deposition first gives a decline while moving from left to right. But then there is a sharp increase in deposition towards the central region of the channel. The maximum deposition is in the range of 5-7% and occurs at the middle potion of channel width but towards the outer region. Once again the deposition rate is less for higher velocity than that for the low velocity. Fig. 6(c) indicates deposition for 8-16μm diameter particles. In this case, there is a gradual variation in depositional pattern starting from approximately 0.5 % at the left bank to a maximum of around 12 % for a velocity of 1 m/sec and 9.5 % for a velocity of 1.5 m/sec. The peak deposition percentage happens at a distance of 300 mm from left end.

Fig. 6(d) depicts the deposition pattern for sediments with particle size range of 16-31μm. Diagram shows that the deposition of particles increases slightly while moving towards the right bank but then there is a sudden decrease towards the outer region. This sharp decline may be attributed to strong secondary circulation existing at the right bank and moving towards the left bank, thus lifting the particles and reducing their deposition quantity. After this, there is gradual increase towards the middle region of the stream and a maximum deposition percentage of 13-14% was observed in the range of 300-350 mm. Once again there is a sharp decline after this peak value and a least deposition percentage happened at the right bank.

Fig. 6(e) shows the percentage of sediment deposition having sizes in the range 31-62µm. The magnitude of peak deposition was around 14% and it happened towards the outer region of the cross section. Fig. 6(f) gives us an idea about siltation of sediments within the range of 62-125µm. It showed that more than 50% of deposition occurred in the middle half of the cross section i.e. half of the total deposited sediment quantity occurred from 125-375mm. The deposition rate is progressively increasing as the sediment sizes are increasing. Initially, the maximum quantity of the sediments remained in suspension and did not settle but moved out of the channel through its outlet. However, with increasing size the deposition quantity is increasing.

Fig. 6(g) also showed approximately the same deposition pattern as that of Fig. 6(f) but with a greater percentage deposition. The peak value was observed against the low velocity of 1 m/sec and it was found to be 22%. This diagram covered the sediments in the range of 125-250µm. Fig. 6(h-i) showed a different deposition behavior than rest of the diagrams. From Fig. 6(h-i) represent deposition pattern for particles in the range 250-500 and 500-1000µm respectively. In these diagrams, there is a very sharp gradient along the cross section from 250-350mm. The upside gradient is the same as that of the downside gradient. The percentage deposited also raised to more than 80% of the total quantity of sediments passing through this cross section. The physical phenomenon

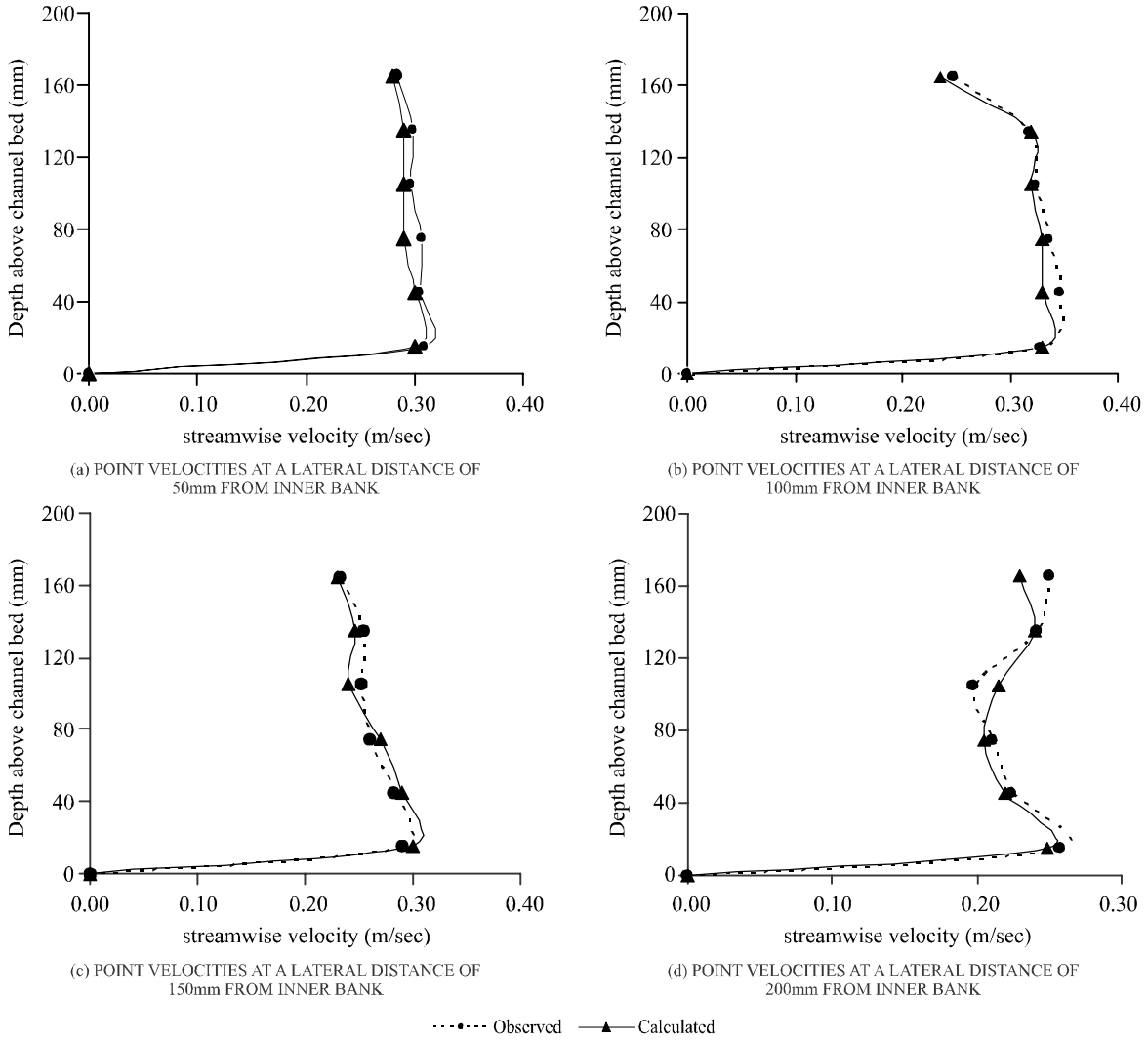

FIG. 5 (a-d). COMPARISON OF OBSERVED AND MODELED DOWNSTREAM POINT VELOCITIES AT APEX E

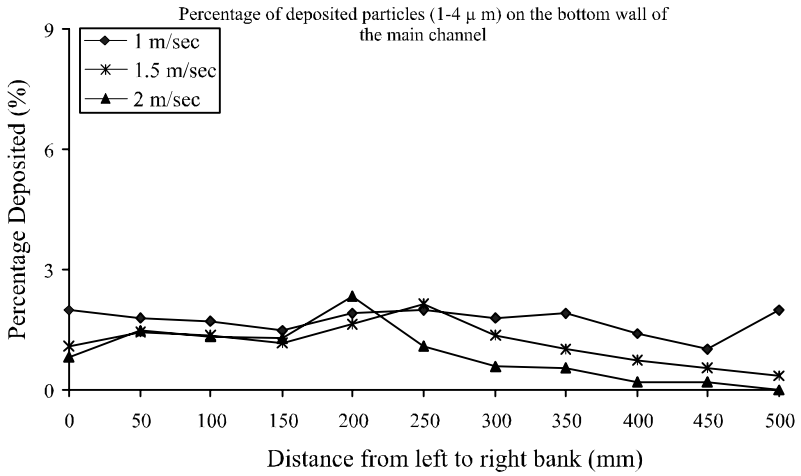

FIG. 6(a). PERCENTAGE OF DEPOSITED SEDIMENTS ACROSS THE WIDTH OF THE CHANNEL

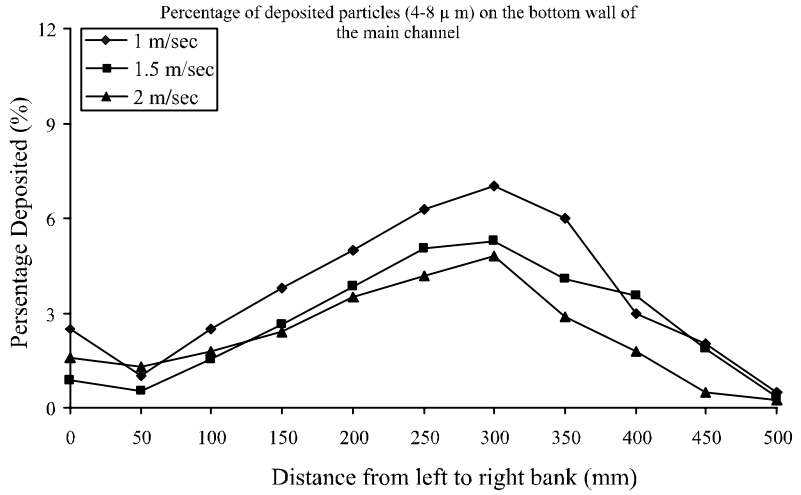

FIG. 6(b). PERCENTAGE OF DEPOSITED SEDIMENTS ACROSS THE WIDTH OF THE CHANNEL

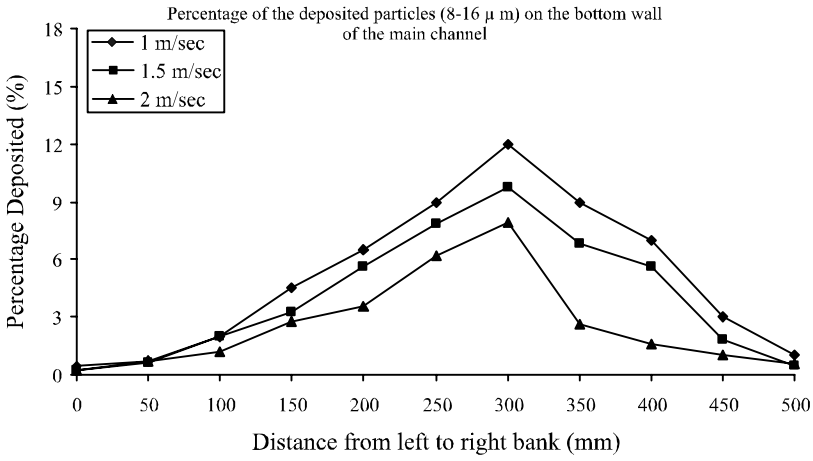

FIG. 6(c). PERCENTAGE OF DEPOSITED SEDIMENTS ACROSS THE WIDTH OF THE CHANNEL

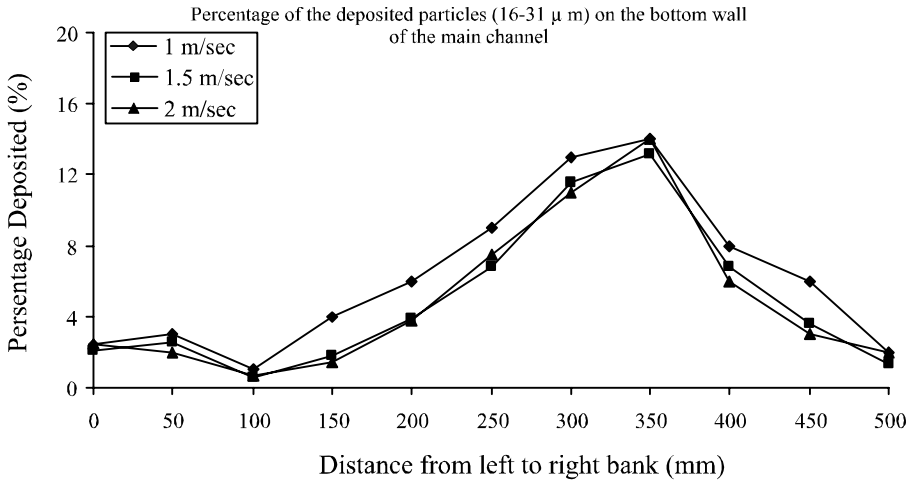

FIG. 6(d). PERCENTAGE OF DEPOSITED SEDIMENTS ACROSS THE WIDTH OF THE CHANNEL.

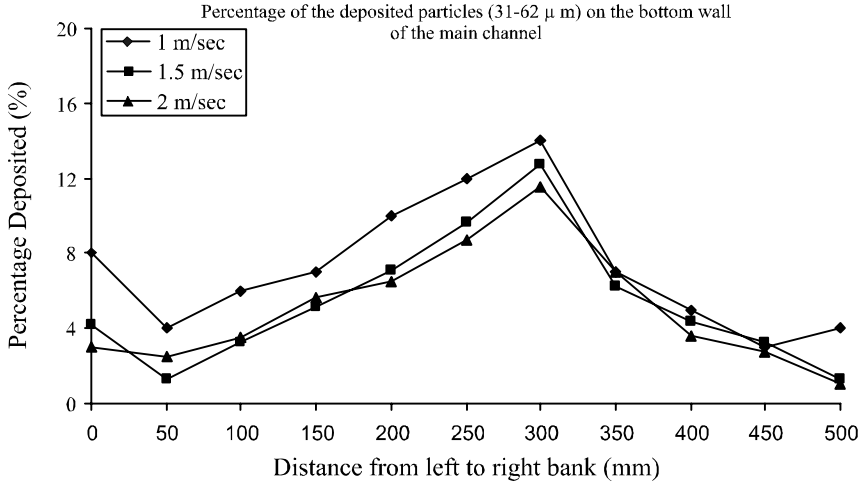

FIG. 6(e). PERCENTAGE OF DEPOSITED SEDIMENTS ACROSS THE WIDTH OF THE CHANNEL

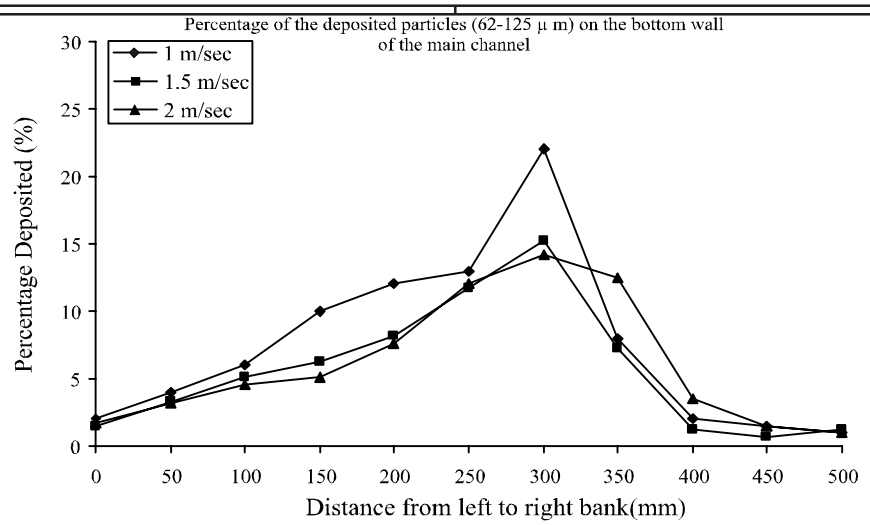

FIG. 6(f). PERCENTAGE OF DEPOSITED SEDIMENTS ACROSS THE WIDTH OF THE CHANNEL

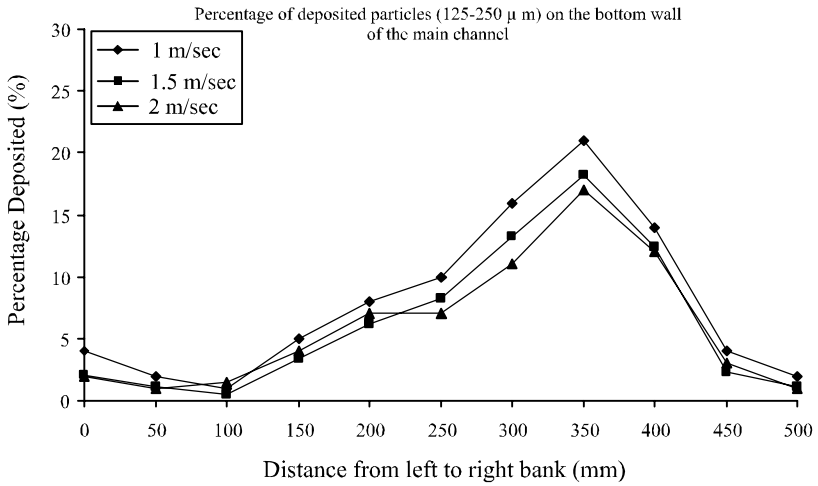

FIG. 6(g). PERCENTAGE OF DEPOSITED SEDIMENTS ACROSS THE WIDTH OF THE CHANNEL

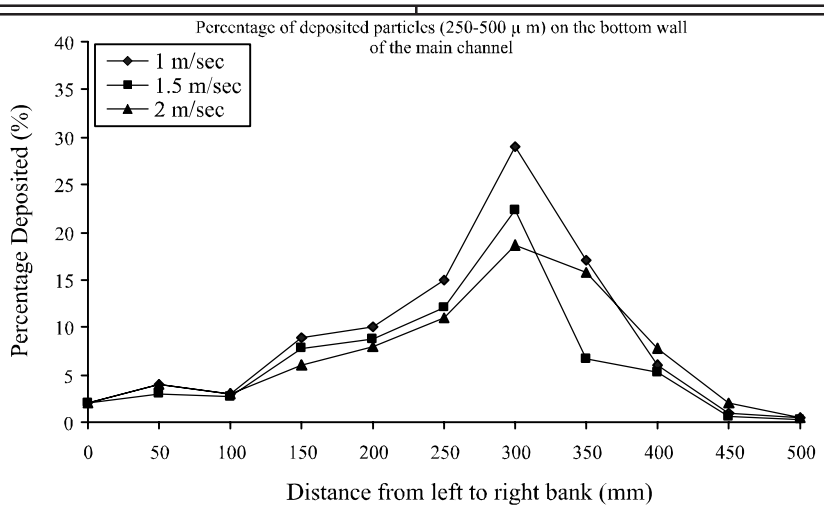

FIG. 6(h). PERCENTAGE OF DEPOSITED SEDIMENTS ACROSS THE WIDTH OF THE CHANNEL

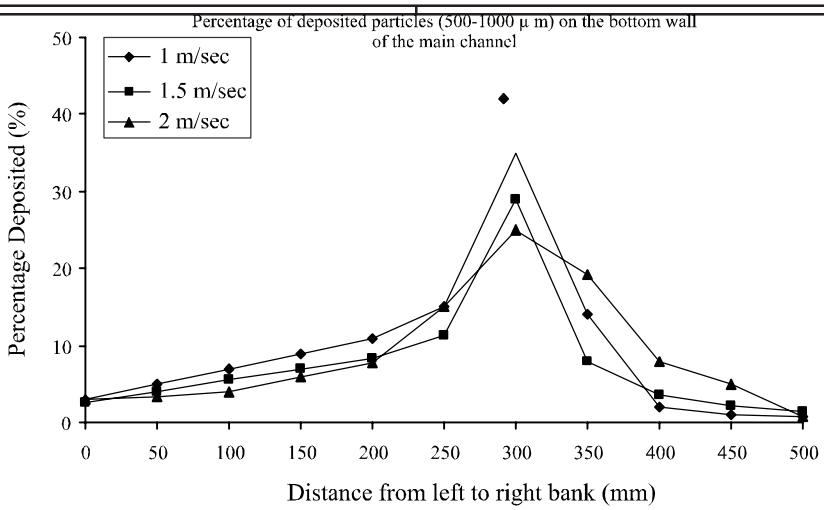

FIG. 6(i). PERCENTAGE OF DEPOSITED SEDIMENTS ACROSS THE WIDTH OF THE CHANNEL

controlling this deposition pattern of the sediments is the boundary shear stress and secondary circulations. The maximum boundary shear stress increases towards the outer bank. The water depth also increases at the outer bank and shows a dip at the inner bank at the apex of the bend. The increase in boundary shear stress and water depth towards outer bank results in accumulation of the coarser bed material in the outer bank region. This is the major reason for enhanced sediment deposition towards outer bank as the diameter of the particles increases. The finer particles are deposited in smaller quantities in the outer region of the x-section due to the presence of strong secondary circulation at the apex. The secondary circulations are developed as follows. When the water remains within the main channel the secondary circulations are pressure driven and are controlled by the centrifugal forces. However, when the water comes overbank the shear driven secondary cells overcome the centrifugal cells with strong intensity towards the outer edge of the section. Thus it can be concluded that the increasing boundary shear stress towards the outer bank and secondary circulations are responsible for (i) deposition of large sized particles towards the outer bank (ii) erosion of sediments very close to the outer bank (iii) lifting and deposition of the small sized particles from outer bank to inner regions of the x-section. All these settlement patterns are clear from the Fig. 6(a-i). The numerical simulation successfully captured this natural deposition phenomenon. The next two diagrams were sketched to get an idea regarding impact of sediment sizes on percentage deposition. The velocity of water was kept constant. The results shown in Fig. 6(j-k). Fig. 6(j-k) show that the deposition quantity changes considerably in the outer regions of the channel.

7. CONCLUSIONS

During the validation process, the simulated results matched closely with the observed (experimental) ones as shown in Figs.4-5. A maximum RMS value of 6% has been observed between experimental and simulated values for discharge calculations whereas for downstream point velocities, the maximum difference is about 8%. This investigation provided us the opportunity to understand the behavior and pattern of deposition of sediment particles of different sizes across a meandering compound channel. It was found that the boundary shear stresses and secondary circulations are responsible for the deposition patterns of the sediments over the cross section. These boundary shear stresses increase towards the outer bank of the apex, thus resulting in accumulation of large %age of large sized particles in this region. On the other hand secondary circulations cause lifting of fine particles from the outer regions. This research work will help us in mitigation of sediment deposition in meandering channels. The design of natural and man-made meandering channels can be improved. It will be helpful in designing proper flushing arrangements of deposited sediments because simulated results can be kept in mind while designing such techniques of flushing.

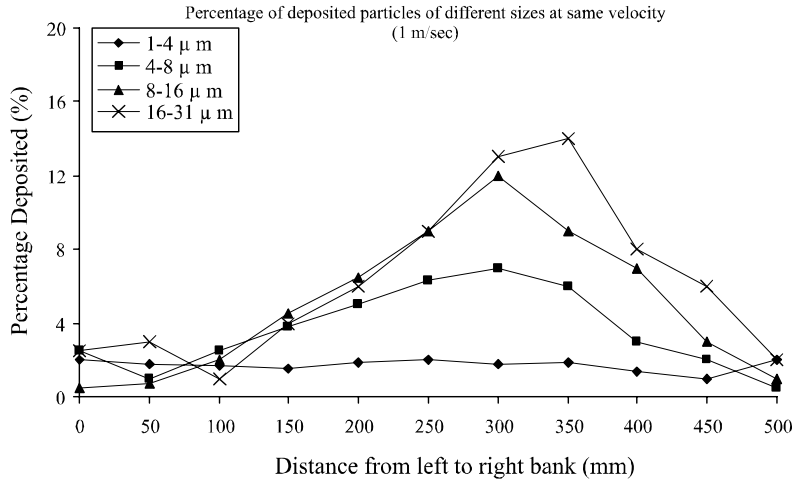

FIG. 6(j). PERCENTAGE OF DEPOSITED SEDIMENTS ACROSS THE WIDTH OF THE CHANNEL

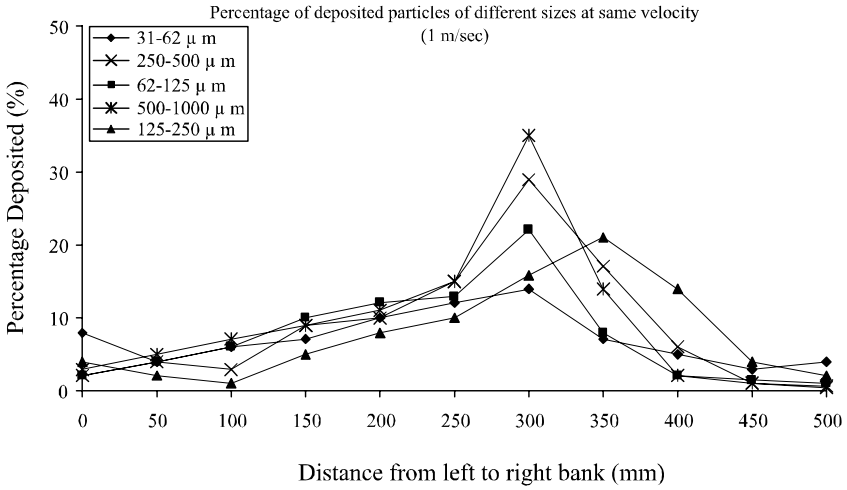

FIG. 6(k). PERCENTAGE OF DEPOSITED SEDIMENTS ACROSS THE WIDTH OF THE CHANNEL

ACKNOWLEDGEMENT

This research work has been conducted using the data of Matin Marriott after getting his permission. This permission is gratefully acknowledged.

REFERENCES

[1] Yilmaz, L., "Experimental Study of Sediment Transport in Meandering Channels", Journal of Water Resources Management, Volume 22, pp. 259-275, Netherlands, 2008.

[2] Toorman, E.A., "Vertical Mixing in the Fully Developed Turbulent Layer of Sediment-Laden Open-Channel Flow", ASCE Journal of Hydraulic Engineering, Volume 134, No. 9, pp. 1225-1235, USA, 2008.

[3] Sharpe, R., and James, C.S., "Deposition of Sediment from Suspension in Emergent Vegetation", Journal of Water SA., Volume 32, No. 2, pp. 211-218, South Africa, 2006.

[4] Mctigue, D.F., "Mixture Theory for Suspended Sediment Transport", ASCE Journal of Hydraulic Division, Volume 107, No. 9, pp. 659-673, USA, 1981.

[5] Widera, P., Toorman, E., and Lacor, C., "Large Eddy Simulation of Sediment Transport in Open Channel Flow", IAHR Journal of Hydraulic Research, Volume 47, No. 3, pp. 291-298, Netherlands, 2009.

[6] Zinke, P., and Olsen, N.R.B., "Modeling of Sediment Deposition in a Partly Vegetated Open Channel", 32nd IAHR Congress, Volume 32, pp. 515-535, Venice, Italy, 2007.

[7] Wilson, C.A.M.E., Guymer, I., Boxall, J.B., and Olsen, N.R.B. "Three-Dimensional Numerical Simulation of Solute Transport in a Meandering Self-Formed River Channel", IAHR Journal of Hydraulic Research, Volume 45, No. 5, pp. 610-616, Netherlands, 2007.

[8] Ahmadi G., and Ma, D., "A Thermo-Dynamical Formulation for the Dispersed Multi-Phased Turbulence Model" International Journal of Multiphase Flow, Volume 16, pp. 323-340, Elsevier, 1990.

[9] Ahmadi G., and Smith, D.H., "Gas Flow and Particle Deposition in the Hot-Gas Filter Vessel at the Tidd 70 MWE PFBC Demonstration Power Plant", Journal of Aerosol Science Technology, Volume 29, pp. 206-223,1998.

[10] "User Guide Fluent 6.3", FLUENT Incorporated, Lebnon.

[11] Rodi, W., “Turbulence Models and Their Applications in Hydraulics”, A State of the art Review, IAHR, Delft, Netherland,1980.

[12] Marriott, M.J., "Hydrodynamics of Flow Around Bends in Meandering and Compound Channels", Ph.D. Thesis, University of Hertfordshire, UK, 1998.

[13] Ruther, N., and Olsen, N.R.B., "Modelling Free Forming Meandering Evolution in a Laboratory Channel Using Three Dimensional Computational Fluid Dynamics", Journal of Geomorphology, Volume 89, pp. 308-319, Elsevier, 2007.

[14] Choi, S.U., Park, M., and Kang, H., "Numerical Simulation of Cellular Secondary Currents and Suspended Sediment Transport in Open-Channel Flows over Smooth-Rough Bed Strips", IAHR Journal of Hydraulic Research, Volume 45, No. 6, pp. 829-840, Netherlands, 2007.

[15] "User Guide Gambit 2.3", FLUENT Incorporated, Lebnon, N.H.